nature photonics

LETTERS

PUBLISHED ONLINE: 19 JANUARY 2014 | DOI: 10.1038/NPHOTON.2013.373

Tip-enhanced infrared nanospectroscopy via molecular expansion force detection

Feng Lu, Mingzhou Jin and Mikhail A. Belkin*

Mid-infrared absorption spectroscopy in the molecular fingerprint region is widely used for chemical identification and quantitative analysis employing infrared absorption spectra databases. The ability to perform mid-infrared spectroscopy with nanometre spatial resolution is highly desirable for applications in materials and life sciences. At present, scattering near-field scanning optical microscopy[1–6] is considered to be the most sensitive technique for nanoscale mid-infrared spectroscopy under ambient conditions. Here, we demonstrate that nanoscale mid-infrared spectra can be obtained with comparable or higher sensitivity by detecting mechanical forces exerted by molecules on the atomic force microscope tip on light excitation. The mechanical approach to mid-infrared nanospectroscopy results in a simple optical set-up that, unlike scattering near-field scanning optical microscopy, requires no cryogenically cooled mid-infrared detectors, is easy to align, and is not affected by sample scattering.

A schematic of the experimental set-up is shown in Fig. 1a. Pulses of tunable infrared light are incident on a sample. Upon optical absorption, molecules transit into an excited vibrational state. In a very short time (~10 ps, ref. 7, much faster than the atomic force microscope (AFM) cantilever response time), the excited vibrational mode non-radiatively dissipates into molecular vibrational modes of lower energies as well as to vibrational and kinetic modes of the surrounding molecules and substrate. Because of the anharmonicity of molecular vibrations, the effective molecular volume increases (on a macroscopic scale this leads to thermal expansion), which results in a force acting on the AFM tip positioned in contact with the sample. This force leads to a small cantilever deflection and subsequent oscillation, which may be detected by the AFM position-sensitive photodetector (PSPD) and amplified by the lock-in amplifier (Fig. 1a). In the first approximation, the force on the AFM tip is linearly proportional to the absorbed optical energy. The dependence of the AFM cantilever deflection Δz on the excitation laser wavelength λ is then expected to follow the molecular absorption $\alpha_{abs}(\lambda)$ after normalization to the incident laser intensity $I(\lambda)$:

$$\frac{\Delta z(\lambda)}{I(\lambda)} \propto \alpha_{abs}(\lambda) \quad (1)$$

The first demonstration that photoexpansion of bulk polymers can be detected by AFM and used for mid-infrared microscopy was carried out by Alexandre Dazzi and co-workers[8], and the theory of the process was developed by the same group in ref. 9. This approach was later extended to imaging of polymer blends[10], biological samples[11] and even electromagnetic modes in nanoresonators[12]. However, only relatively thick samples (~15 nm thick or thicker[13,14]) produced detectable cantilever deflections, even when the mid-infrared laser power was close to thermal sample damage and the spatial resolution was limited, in a first approximation, by the thermal diffusion length in samples during a short laser pulse[8–14]. Here, we show that the sensitivity of mid-infrared photoexpansion nanospectroscopy may be improved by several orders of magnitude and that the nanoscale images can be taken with a spatial resolution effectively limited only by the AFM tip apex size. We report high-quality mid-infrared spectra collected from samples as small as monolayer islands and attain a sensitivity exceeding that obtained by the best scattering near-field scanning optical microscopy (s-NSOM) systems[1,2].

To detect the minute amount of force produced by the expansion of a few molecules below the AFM tip, we first exploit mechanical resonant enhancement of the cantilever deflection amplitude. This is achieved by matching the repetition frequency of laser pulses with a resonant frequency of one of the bending modes of the cantilever. We use broadly tunable mid-infrared quantum cascade lasers (QCLs) as light sources, because their pulse repetition frequency can be controlled easily by current pulses through the laser[15,16]. The cantilever deflection amplitude is then amplified by the quality factor (Q-factor) of a particular mode, which is ~100 for the commercially available silicon cantilevers used in our set-up but may be as high as 5×10^3 in air for tuning-fork-based cantilevers[17].

However, mechanical resonance enhancement alone is not sufficient to produce monolayer sensitivity in our experiments, as shown in our previous report[16]. To achieve submonolayer sensitivity we also use electromagnetic enhancement of the optical field intensity in the nanogap between a sharp gold-coated AFM tip and a gold-coated substrate. Figure 1b shows the simulation of field intensity enhancement for a monolayer sample. For a 2-nm-thick sample representative of a typical monolayer thickness[18], the enhancement factor is calculated to be as high as 2×10^5 (Fig. 1b). Local field intensity enhancement effectively increases the mid-infrared absorption cross-section of molecules under the AFM tip by over five orders of magnitude and also improves the spatial resolution of our microscopy, which is now determined only by the dimensions of the 'hot spot' under the AFM tip.

For experimental demonstration, self-assembled monolayers (SAMs) were prepared on template-stripped gold (TSG) substrates[19]. Two SAMs were tested: one made of relatively large hydroxyl-terminated hexa (ethylene glycol) undecanethiol molecules (EG6-OH) and one made of small 4-nitrothiophenol molecules (NTP). The molecular structures for both compounds are described in the Methods. Thiolated SAMs have a high affinity to the surfaces of noble metals like gold and silver[18]. The assembled EG6-OH monolayer had a thickness of ~1.5 nm, as confirmed by AFM topographic measurement, while the thickness of the NTP monolayer was below the topographic detection limit of our set-up and was estimated to be substantially smaller than 1 nm.

The p-polarized mid-infrared pulses from a tunable QCL were incident on the sample. Their repetition frequency was carefully

Department of Electrical and Computer Engineering, Microelectronics Research Center, The University of Texas at Austin, 10100 Burnet Road, Austin, Texas 78758, USA. *e-mail: mbelkin@ece.utexas.edu

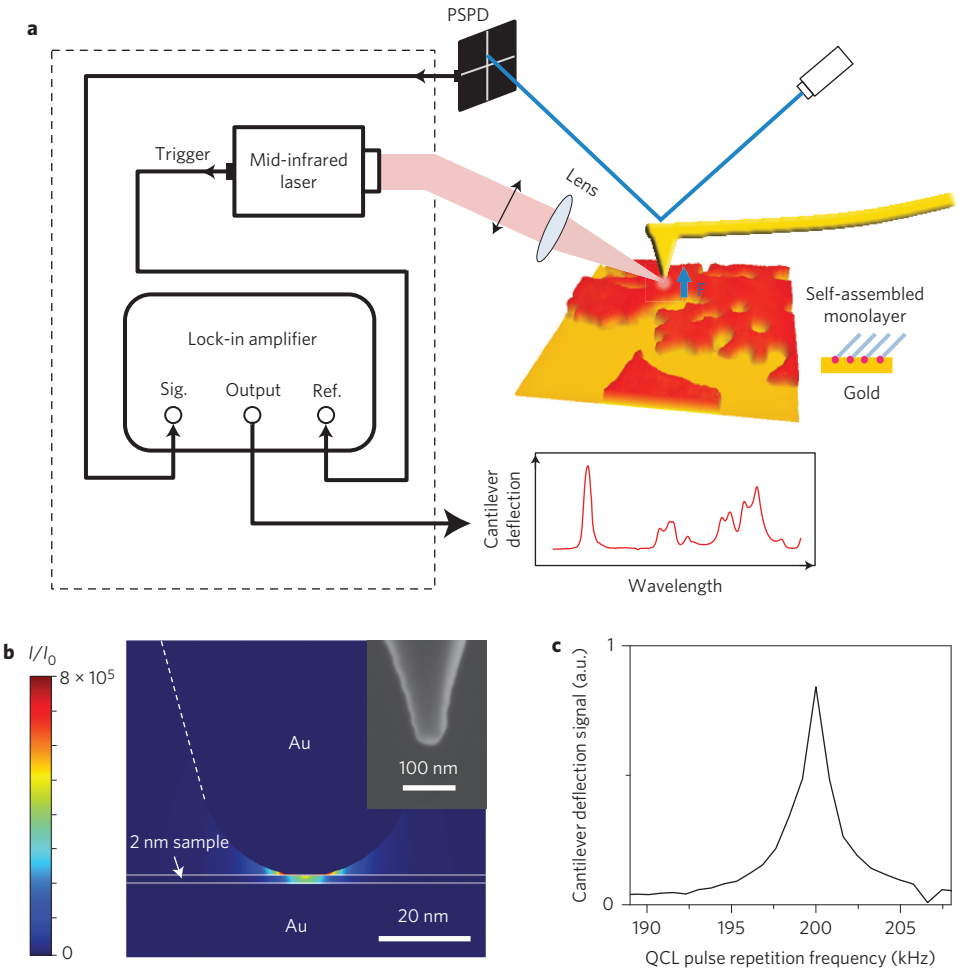

Figure 1 | Description of experiment. a, Schematic of the experimental set-up, in which p-polarized light pulses from a mid-infrared laser are focused on a sample. Cantilever deflection due to the molecular force action is detected by a position-sensitive photodetector (PSPD). The PSPD signal is sent to the lock-in amplifier referenced by the laser pulse repetition frequency. The amplifier output is a measure of the cantilever oscillation amplitude at the lock-in reference frequency. **b**, Three-dimenisonal simulation of the tip-enhancement of the light intensity (I/I_0) for a 2-nm-thick molecular monolayer on gold. The mid-infrared light is incident at 75° to the surface normal, as in the experiment. The AFM tip was modelled to have a radius of curvature of 25 nm and a half-cone angle of 17°, similar to the actual geometry seen in the scanning electron micrograph (inset). See Supplementary Section I for other simulation parameters. **c**, Experimental dependence of the lock-in output on the repetition frequency of QCL pulses. The data show a resonant peak at the cantilever second bending mode frequency in contact with the sample. The *Q*-factor is estimated from the peak linewidth to be 93.

maintained to match the second bending mode of the AFM cantilever at ~200 kHz (Fig. 1c). The dependence of the cantilever deflection amplitude on laser wavelength is shown in blue in Fig. 2a,b for the two SAM samples. We call these curves 'photoexpansion spectra' because the spectral features are produced by forces due to molecular expansion under the AFM tip. The data were normalized to the QCL light intensity as shown in equation (1). Figure 2 also shows reference absorption spectra measured by the mid-infrared reflection–absorption spectroscopy for the same monolayer material on gold in refs 20 and 21. The photoexpansion spectra are in excellent agreement with the absorption spectra.

For EG6-OH, the absorption bands centred at 1,345 cm^{-1} and 1,244 cm^{-1} correspond to CH_2 wagging and twisting modes, respectively[20]. Owing to the limited tuning range of our QCL source, only part of the stronger C − O − C stretching band (peak at 1,130 cm^{-1}) was measured. For NTP molecules, a strong peak around 1,339 cm^{-1}, which corresponds to the symmetric NO_2 stretching mode, can be clearly seen. We also observed a much weaker absorption band around ~1,175–1,183 cm^{-1} due to vibration of the benzene ring. The NTP results demonstrate our ability to collect mid-infrared spectra from small molecules.

High spatial resolution is demonstrated with a sample made of monolayer islands of poly(ethylene glycol) methyl ether thiol (PEG) on TSG. PEG molecules have a backbone structure similar to that of EG6-OH with its CH_2 wagging mode peaked at 1,342 cm^{-1}, and could form small islands on TSG substrates. The island height is ~2 nm, as confirmed by the topographic measurement in Fig. 3a. Figure 3b displays a topographic line scan along the blue arrow shown in Fig. 3a. We positioned the AFM tip at different points along the line scan (marked with squares in Fig. 3b) and collected photoexpansion spectra at these locations. The results are shown in Fig. 3c, where the spectra are colour-coded and numbered to correspond to the measurement position markers in Fig. 3b. We can distinguish PEG islands from bare gold by monitoring the CH_2 wagging band with a spatial resolution better than 30 nm. Figure 3d compares the dependence of the cantilever deflection signal along the line scan in Fig. 3b where the laser frequency is set to the 1,342 cm^{-1} absorption line of PEG and to 1,352 cm^{-1}, away from the absorption line. As expected, the contrast between PEG and gold is only observed at 1,342 cm^{-1}.

The mid-infrared chemical mapping capability of PEG islands is demonstrated in Fig. 3e. For this case we fixed the laser frequency at

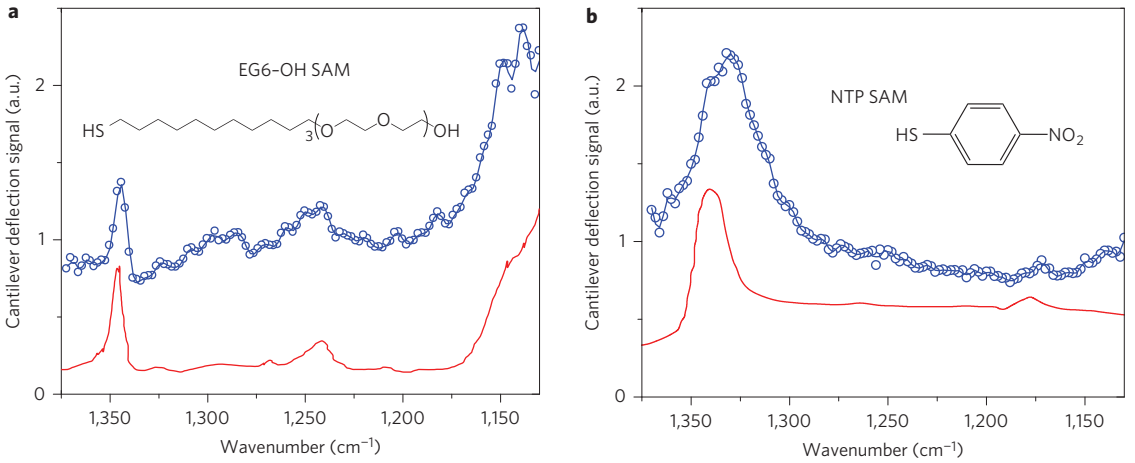

Figure 2 | Photoexpansion spectra of self-assembled monolayers on gold. a, EG6-OH. **b**, NTP. Blue circles are measured data. Data points are connected by B-splines to guide the eye. Red curves are the mid-infrared reflection–absorption spectra of corresponding SAMs taken for **a** (from ref. 20) and for **b** (from ref. 21). Insets: molecular structure of the samples. Red curve in Fig. 2a redrawn with permission from ref. 20, © 1998 ACS; red curve in Fig. 2b redrawn with permission from ref. 21, © 1999 OSA.

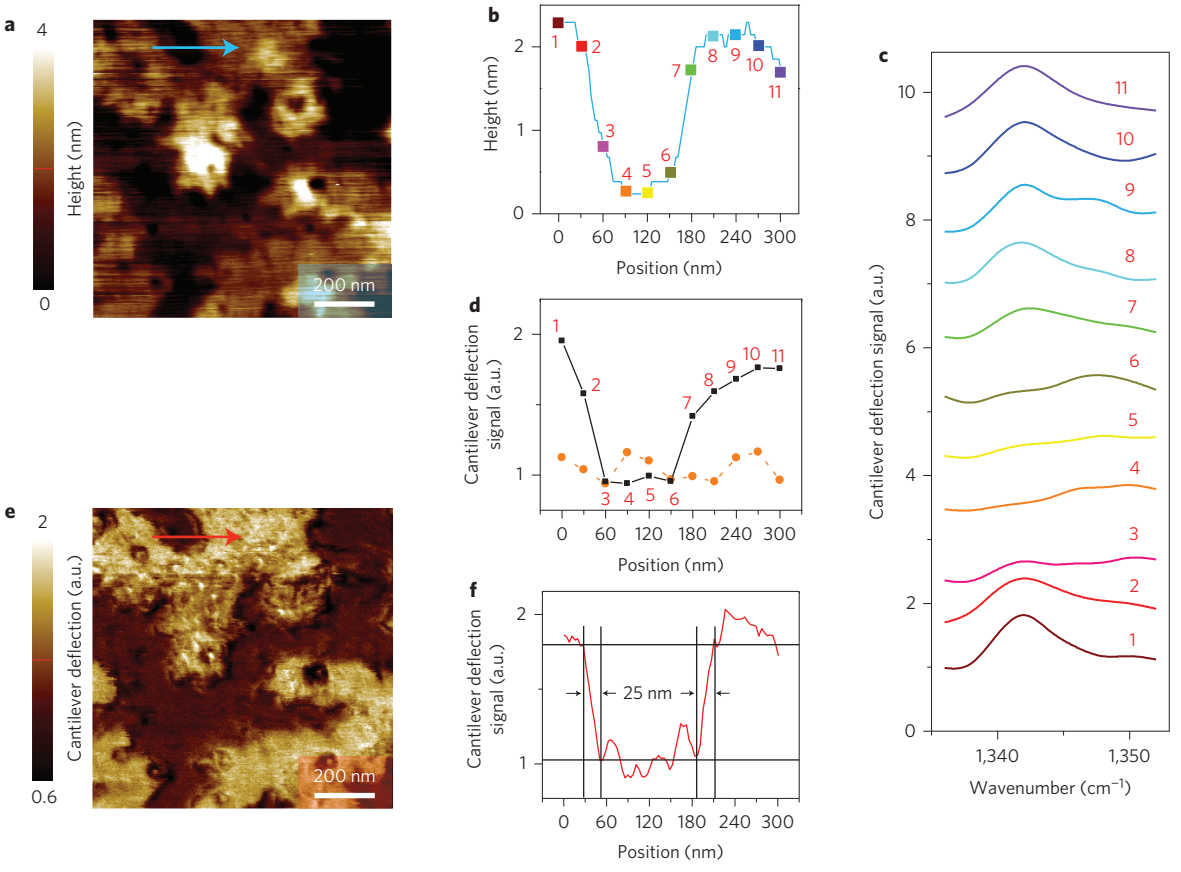

Figure 3 | Demonstration of spatial resolution. a, Topography of the PEG monolayer islands acquired in contact mode. **b**, Topographic line scan along the blue arrow in **a**, showing the height of the monolayer islands to be ~2 nm. Square symbols mark positions where the photoexpansion spectroscopy measurements were performed. **c**, Mid-infrared photoexpansion spectra taken at the positions indicated in **b**. The curves are labelled and coloured in accordance with **b**. Spectra are offset vertically for clarity. **d**, Cantilever deflection signal at different points along the topographic scan in **b** for the laser tuned to the 1,342 cm^{-1} PEG absorption line (black squares connected by a black solid line) and to 1,552 cm^{-1}, away from the PEG absorption line (orange circles connect by a dashed orange line). Data points are extracted from spectra in **c**. **e**, Mid-infrared mapping of monolayer islands: the lock-in output is recorded as a function of tip position for the mid-infrared laser wavelength fixed at the PEG CH_2 wagging absorption band at 1,342 cm^{-1}. Bright regions are PEG molecules and dark regions are gold. The image has 256 × 256 pixels and was obtained simultaneously with the topographic image in Fig. 3a. The image was produced by raster scanning at a rate of 0.5 Hz with the lock-in integration time set to 3 ms. The total acquisition time was ~5 min. **f**, Signal along the line scan shown with a red arrow in **e**. Data indicate a spatial resolution of ~25 nm for the image in **e**.

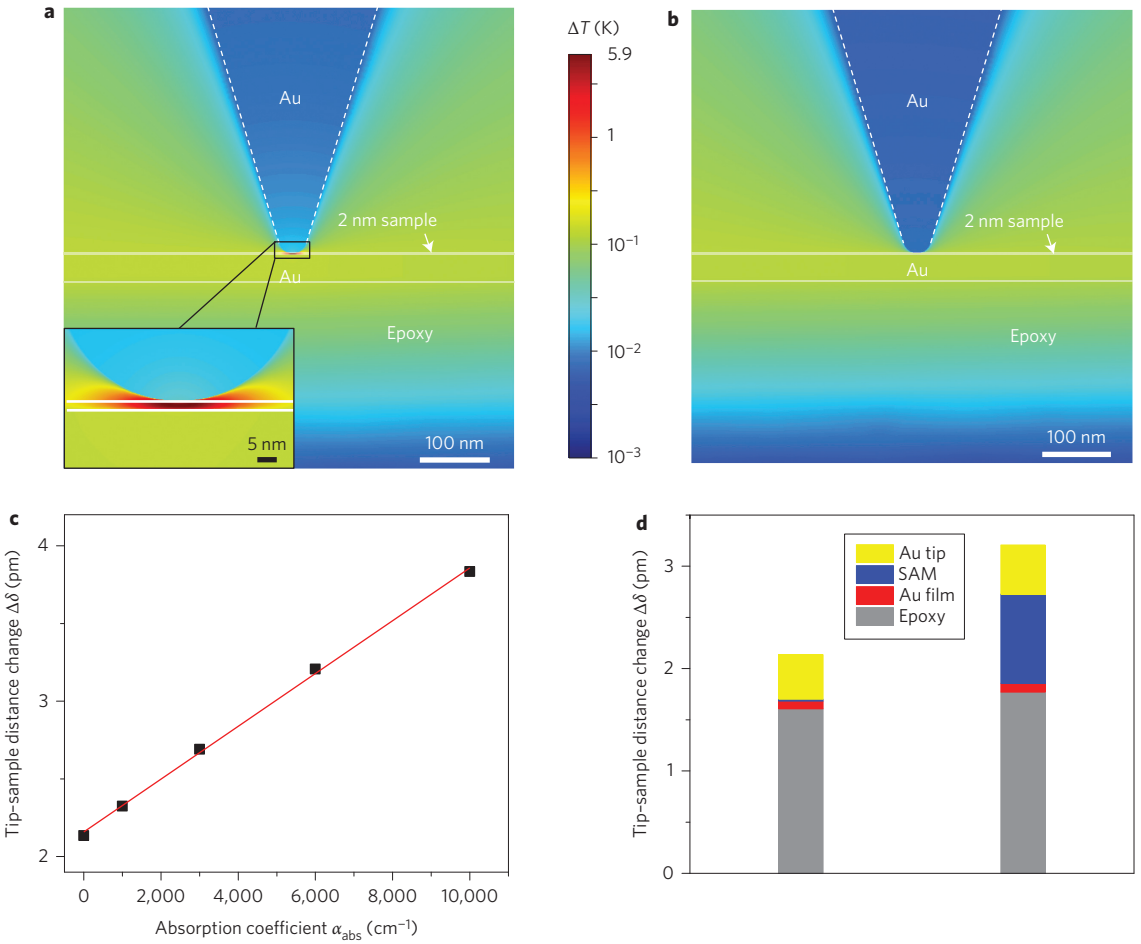

Figure 4 | Sample heating and expansion. a, Temperature increase at the end of a 160-ns-long pulse in and around a monolayer sample below the AFM tip. The monolayer is assumed to have an absorption coefficient $\alpha_{abs} = 6{,}000\ cm^{-1}$, which corresponds to absorption in PEG and EG6-OH samples at $1{,}342\ cm^{-1}$. **b**, Temperature increase at the end of a 160-ns-long pulse in and around a non-absorbing monolayer sample below the AFM tip. **c**, Dependence of tip–sample distance change $\Delta\delta$ due to sample expansion caused by a mid-infrared pulse. **d**, Histograms showing the accumulated sample expansion from monolayer, substrate and tip for $\alpha_{abs} = 0\ cm^{-1}$ (left) and $\alpha_{abs} = 6{,}000\ cm^{-1}$ (right). The incident infrared pulse was assumed to have a peak power of 500 mW and to be focused to a 100-μm-radius spot for the simulations, similar to the experimental situation.

the PEG absorption peak at $1{,}342\ cm^{-1}$ and recorded the AFM cantilever deflection amplitude as a function of tip position. The mid-infrared mapping image shows a clearer contrast and more detail compared to the topographic image of the same sample section shown in Fig. 3a. From the data in Fig. 3f, we estimate the spatial resolution to be better than 25 nm, limited by the apex size of the AFM tip used in our experiments.

We estimate that ~300 molecules contribute to cantilever deflection in our experiments. This number is based on the simulated intensity hot-spot diameter of ~10 nm (Fig. 1b) and the molecular density of 4 molecules nm^{-2} (ref. 20). Given the signal-to-noise ratio in the spectra shown in Fig. 2, we expect to be able to see strong absorption peaks from as few as 30 molecules below the tip. The sensitivity can potentially be increased further by using sharper AFM tips that provide higher intensity enhancement, similar to that used for tip-enhanced Raman spectroscopy[22–24], and AFM cantilevers with higher Q-factors. Even at this present stage, the mid-infrared spectra reported here are of higher quality than the mid-infrared spectra produced by the state-of-the-art s-NSOM for monolayer or thin-film samples[1,2].

Figure 4a,b presents the simulated temperature distribution in and around the monolayer sample at the end of a 160-ns-long light pulse in the case where the monolayer is absorbing (Fig. 4a) and non-absorbing (Fig. 4b). Sample heating is estimated to be below 6 K based on the results of the COMSOL simulations shown in Fig. 4a. The low values of simulated sample heating are in agreement with an experimental observation that no signal degradation is observed for same-point measurements and that both spectral and topographic measurements are repeatable over the same sample areas.

Assuming bulk values of thermal expansion for all materials, we may estimate the tip–distance change $\Delta\delta$ due to sample light absorption and sample expansion in both cases (Fig. 4c). We note that $\Delta\delta$ scales linearly with absorption in the monolayer (red line in Fig. 4c), with a significant background level due to residual light absorption in the gold-coated substrate and the AFM tip (Fig. 4d). Because the optical properties of gold are virtually constant in the experiment spectral range, the background is expected to be spectrally flat. The experimental spectrum in Fig. 2a indeed shows a flat background signal with a ratio of the $1{,}345\ cm^{-1}$ peak to the background level of ~1.7, which is in good agreement with the theoretical prediction of 1.5 in Fig. 4c.

The absorption-induced mechanical force on the tip, F_{abs}, is deduced using the Derjaguin–Muller–Toporov (DMT) model of sample–tip interaction[25,26]. Although the validity of macroscopic models for nanoscale contact is yet to be determined[27], the model explains the key experimental results well. Assuming $\Delta\delta \ll \delta$, where δ is the indentation depth in the sample in contact mode,

we obtain

$$F_{abs} \approx 2E^* R^{1/2} \delta^{1/2} \Delta\delta \quad (2)$$

where R is the radius of the tip apex and E^* is the reduced elastic modulus of the sample. Taking from ref. 28 the mechanical parameters for a SAM that is similar to our EG6-OH and PEG samples, we obtain $\delta \approx 0.7$ nm and $F_{abs} \approx 0.13$ nN for $\Delta\delta = 3.2$ pm (taken from Fig. 4d). The value of F_{abs} may be used to estimate the expected cantilever deflection and compare it with experiment. We obtain a theoretical value of the cantilever deflection amplitude of 0.1 nm for the second mechanical bending mode. The number is in good agreement with the experimental $z \approx$ 0.25 nm deduced from the strength of the PSPD signal. Details of this analysis are provided in Supplementary Section III.

As well as F_{abs}, electromagnetic forces may also affect cantilever deflection[29]. We evaluated the optical force on the tip in COMSOL using Maxwell's stress tensor for experimental conditions with 500 mW laser power focused onto a 100-μm-radius spot below the tip (cf. Fig. 1b). We obtained $F_{opt} \approx 0.3$ pN $\ll F_{abs}$. We also note that, unlike F_{abs}, F_{opt} is virtually independent of the absorption coefficient of the monolayer film. Thus, it is the mechanical force action on the AFM tip that produces spectral signatures in our experiments.

In conclusion, we have demonstrated that mid-infrared vibrational spectra of molecular monolayers and monolayer islands could be collected under ambient conditions with high sensitivity and better than 25 nm spatial resolution by detecting the mechanical force exerted on an AFM tip by molecules excited with pulses of mid-infrared radiation. Approximately 300 molecules are interacting with the AFM tip in our experiments, and the set-up sensitivity is estimated to be ~30 molecules. Mid-infrared spectra obtained by detecting mechanical molecular action show higher sensitivity than those obtained by the best s-NSOM systems[1,2] applied to similar or thicker samples. In contrast to s-NSOM, the mechanical approach to mid-infrared nanospectroscopy relies on a simple optical set-up that has no cryogenically cooled mid-infrared detectors, is easy to align and is not affected by sample scattering.

Methods

Measurements. A pulsed broadly tunable QCL (ÜT-8, Daylight Solutions) with a spectral range 1,130–1,375 cm^{-1} was used in the experiments. The laser provided 160 ns light pulses at variable repetition frequency. The p-polarized light was incident from above the sample at an angle of ~75° to the surface normal and focused to a 100-μm-radius spot on the sample. The laser peak power was in the range 100–800 mW depending on the wavelength of operation. The photoexpansion spectra were obtained by normalizing the lock-in output signal from a sample to that from a clean TSG substrate. We confirmed that the signal from the latter followed the dependence of the laser peak power on wavelength (Supplementary Fig. 3).

A commercial AFM system was placed on a vibrational insulation platform without using any acoustic insulation. The AFM was operated in contact mode with a setpoint of 10 nN. The QCL pulse repetition frequency was maintained in resonance with the second bending mode of a gold-coated AFM cantilever at ~200 kHz. The second bending mode was chosen empirically from four cantilever bending mode resonances accessible with our QCL source as the one that enabled imaging and spectroscopy with the highest signal-to-noise ratio. The radius of curvature of the tip apex was ~25 nm. The deflection signal from the PSPD ('A–B' signal) was amplified with a lock-in amplifier using an integration time of 30 ms. The spectra in Figs 2 and 3 were measured with a spectral resolution of 2 cm^{-1} by stepping the QCL external grating every 1.5 s. A full spectrum in Fig. 2 took ~6 min, mostly limited by the time required to stabilize the laser grating after each spectral step. The actual signal collection time was only ~30 ms × 121 data points ≈ 3.6 s. Recently, in collaborating with the group of Prof. Bernhard Lendl, we were able to obtain similar spectra in only 2 s, using continuous-tuning of QCLs, as described in ref. 30.

Sample preparation. TSG substrates were fabricated according to ref. 19 with some modification. The 50 × 75 mm highest-grade V1 mica sheets (Ted Pella) were freshly cleaved and immediately mounted inside the chamber of an electron-beam evaporation system. A 40-nm-thick gold layer was deposited at a rate of 0.5 Å s^{-1} and a pressure of 8×10^{-6} mbar. The gold–mica sheets were then annealed in an oven for 2 h at 300 °C in a nitrogen environment. The sheets were cleaved into smaller pieces (20 × 20 mm), with the gold surface glued onto silicon pieces of similar size using EPO-TEK 377 (Epoxy Technology) and cured on a hot plate at 150 °C for 1 h. To expose the gold surface, we simply broke the silicon substrate and carefully peeled the mica off by hand. A large surface of gold was routinely obtained with very little mica residue. The conductivity was checked with an ohm-meter. The root-mean-square roughness of the gold surface was measured to be ~3 Å for an area of 5 × 2.5 μm by an AFM in tapping mode. Small holes on the gold films sometimes appeared (see, for example, Fig. 3a) due to a non-optimized procedure.

EG6-OH (molecular formula $HS(CH_2)_{11}(OCH_2CH_2)_6OH$; molecular mass, 468.69 Da) was purchased from Obiter Research. NTP ($HSC_6H_4NO_2$, 155.17 Da) and PEG ($HS(CH_2)_2(OCH_2CH_2)_{21}OCH_3$, 1,000 Da) were purchased from Sigma-Aldrich. All materials were used as received. To prepare a SAM sample of EG6-OH and NTP, the TSG substrates were immersed in a ~1 mM l^{-1} ethanolic solution for ~24 h and then rinsed with a copious amount of 200-proof ethanol and dried in a stream of nitrogen gas. To prepare the monolayer island sample of PEG, the TSG substrates were immersed in a ~1 mM l^{-1} ethanolic solution for appropriate short periods and then rinsed and dried as above.

Received 27 June 2013; accepted 12 December 2013; published online 19 January 2014

References

1. Huth, F. *et al.* Nano-FTIR absorption spectroscopy of molecular fingerprints at 20 nm spatial resolution. *Nano Lett.* **12,** 3973–3978 (2012).
2. Xu, X. G., Rang, M., Craig, I. M. & Raschke, M. B. Pushing the sample-size limit of infrared vibrational nanospectroscopy: from monolayer toward single molecule sensitivity. *J. Phys. Chem. Lett.* **3,** 1836–1841 (2012).
3. Huth, F., Schnell, M., Wittborn, J., Ocelic, N. & Hillenbrand, R. Infrared-spectroscopic nanoimaging with a thermal source. *Nature Mater.* **10,** 352–356 (2011).
4. Knoll B. & Keilmann F. Near-field probing of vibrational absorption for chemical microscopy. *Nature* **399,** 134–137 (1999).
5. Hillenbrand, R., Taubner, T. & Keilmann, F. Phonon-enhanced light–matter interaction at the nanometre scale. *Nature* **418,** 159–162 (2002).
6. Brehm, M., Taubner, T., Hillenbrand, R. & Keilmann, F. Infrared spectroscopic mapping of single nanoparticles and viruses at nanoscale resolution. *Nano Lett.* **6,** 1307–1310 (2006).
7. Puttkamer, K. V., Dubal, H.-R. & Quack, M. Time-dependent processes in polyatomic molecules during and after intense infrared irradiation. *J. Chem. Soc. Faraday Discuss.* **75,** 197–210 (1983).
8. Dazzi, A., Prazeres, R., Glotin, F. & Ortega, J. M. Local infrared microspectroscopy with subwavelength spatial resolution with an atomic force microscope tip used as a photothermal sensor. *Opt. Lett.* **30,** 2388–2390 (2005).
9. Dazzi, A., Glotin, F. & Carminati, R. Theory of infrared nanospectroscopy by photothermal induced resonance. *J. Appl. Phys.* **107,** 124519 (2010).
10. Dazzi, A. *et al.* AFM–IR: combining atomic force microscopy and infrared spectroscopy for nanoscale chemical characterization. *Appl. Spectrosc.* **66,** 1365–1384 (2012).
11. Policar, C. *et al.* Subcellular IR imaging of a metal–carbonyl moiety using photothermally induced resonance. *Angew. Chem. Int. Ed.* **50,** 860–864 (2011).
12. Lahiri, B., Holland, G., Aksyuk, V. & Centrone, A. Nanoscale imaging of plasmonic hot spots and dark modes with the photothermal-induced resonance technique. *Nano Lett.* **13,** 3218–3224 (2013).
13. Felts, J. R. *et al.* Atomic force microscope infrared spectroscopy on 15 nm scale polymer nanostructures. *Rev. Sci. Instrum.* **84,** 023709 (2013).
14. Lahiri, B., Holland, G. & Centrone, A. Chemical imaging beyond the diffraction limit: experimental validation of the PTIR technique. *Small* **9,** 439–445 (2013).
15. Troccoli, M. *et al.* High-performance quantum cascade lasers grown by metal–organic vapor phase epitaxy and their applications to trace gas sensing. *J. Lightwave Technol.* **26,** 3534–3555 (2008).
16. Lu, F. & Belkin, M. A. Infrared absorption nano-spectroscopy using sample photoexpansion induced by tunable quantum cascade lasers. *Opt. Express* **19,** 19942–19947 (2011).
17. Hida, H. *et al.* Fabrication of a quartz tuning-fork probe with a sharp tip for AFM systems. *Sens. Actuat. A* **148,** 311–318 (2008).
18. Love, J. C., Estroff, L. A., Kriebel, J. K., Nuzzo, R. G. & Whitesides, G. M. Self-assembled monolayers of thiolates on metals as a form of nanotechnology. *Chem. Rev.* **105,** 1103–1169 (2005).
19. Hegner, M., Wagner, P. & Semenza, G. Ultralarge atomically flat template-stripped Au surfaces for scanning probe microscopy. *Surf. Sci.* **291,** 39–46 (1993).
20. Harder, P., Grunze, M., Dahint, R., Whitlesides, G. M. & Laibinis, P. E. Molecular conformation in oligo(ethylene glycol)-terminated self-assembled monolayers on gold and silver surfaces determines their ability to resist protein adsorption. *J. Phys. Chem. B* **102,** 426–436 (1998).
21. Merklin, G. T., He, L.-T. & Griffiths, P. R. Surface-enhanced infrared absorption spectrometry of p-nitrothiophenol and its disulfide. *Appl. Spectrosc.* **53,** 1448–1453 (1999).

22. Steidtner, J. & Pettinger, B. Tip-enhanced Raman spectroscopy and microscopy on single dye molecules with 15 nm resolution. *Phys. Rev. Lett.* **100,** 236101 (2008).
23. Zhang, W., Yeo, B. S., Schmid, T. & Zenobi, R. Single molecule tip-enhanced Raman spectroscopy with silver tips. *J. Phys. Chem. C* **111,** 1733–1738 (2007).
24. Neacsu, C. C., Dreyer, J., Behr, N. & Raschke, M. B. Scanning-probe Raman spectroscopy with single-molecule sensitivity. *Phys. Rev. B* **73,** 193406 (2006).
25. Derjaguin, B. V., Muller, V. M. & Toporov, Y. P. Effect of contact deformations on the adhesion of particles. *J. Colloid Interface Sci.* **53,** 314–326 (1975).
26. Israelachvili, J. N. *Intermolecular and Surface Forces* (Academic, 2003).
27. Luan, B. & Robbins, M. O. The breakdown of continuum models for mechanical contacts. *Nature* **435,** 929–932 (2005).
28. DelRio, F. W., Jaye, C., Fischer, D. A. & Cook, R. F. Elastic and adhesive properties of alkanethiol self-assembled monolayers on gold. *App. Phys. Lett.* **94,** 131909 (2009).
29. Kohlgraf-Owens, D. C., Sukhov, S. & Dogariu, A. Mapping the mechanical action of light. *Phys. Rev. A* **84,** 011807(R) (2011).
30. Brandstetter, M. & Lendl, B. Tunable mid-infrared lasers in physical chemosensors towards the detection of physiologically relevant parameters in biofluids. *Sens. Actuat. B* **170,** 189–195 (2012).

Acknowledgements

The authors acknowledge financial support from the Robert A. Welch Foundation (grant no. F-1705) and the US Department of Energy STTR program. Sample fabrication was carried out in the Microelectronics Research Center at the University of Texas at Austin, which is a member of the National Nanotechnology Infrastructure Network (NNIN). The authors thank C. Prater, V. Yakovlev and F. Lagugné-Labarthet for discussions.

Author contributions

M.A.B. conceived and designed the experiments. F.L. built the experimental set-up. F.L. and M.J. performed the experiments. All authors analysed the data and wrote the paper.

Additional information

Supplementary information is available in the online version of the paper. Reprints and permissions information is available online at www.nature.com/reprints. Correspondence and requests for materials should be addressed to M.A.B.

Competing financial interests

M.A.B. and F.L. are co-authors of US patent application no. 13/307,464, 'High frequency deflection measurement of IR absorption'. M.J. declares no competing financial interests.